

<https://helda.helsinki.fi>

---

## Comparison of repulsive interatomic potentials calculated with an all-electron DFT approach with experimental data

Zinoviev, A. N.

2017-09-01

---

Zinoviev , A N & Nordlund , K 2017 , ' Comparison of repulsive interatomic potentials calculated with an all-electron DFT approach with experimental data ' , Nuclear Instruments & Methods in Physics Research. Section B: Beam Interactions with Materials and Atoms , vol. 406 , pp. 511-517 . <https://doi.org/10.1016/j.nimb.2017.03.047>

---

<http://hdl.handle.net/10138/308768>

<https://doi.org/10.1016/j.nimb.2017.03.047>

---

cc\_by\_nc\_nd

acceptedVersion

---

*Downloaded from Helda, University of Helsinki institutional repository.*

*This is an electronic reprint of the original article.*

*This reprint may differ from the original in pagination and typographic detail.*

*Please cite the original version.*

# Comparison of DMol interatomic potentials with experimental data

A.N. Zinoviev <sup>a</sup>, K.Nordlund <sup>b</sup>

<sup>a</sup> *Ioffe Institute, 194021, St.Petersburg, Russia*

<sup>b</sup> *Department of Physics, P.O. Box 43, FIN -00014, University of Helsinki, Helsinki, Finland*

The interatomic potential determines the nuclear stopping power in materials. Most ion irradiation simulation models are based on the universal ZBL interatomic potential, which, however, is an average and hence may not describe the stopping of all ion-material combinations well. Here we consider pair-specific interatomic potentials determined experimentally and by density-functional theory simulations with the DMol approach using numerical, all-electron basis sets. The interatomic potentials calculated using the DMol approach demonstrate an unexpectedly good agreement with experimental data. Differences are mainly observed for heavy atom systems, which suggests they can be improved by extending a basis set and more accurately considering the relativistic effects. Experimental data prove that the approach of determining interatomic potentials from quasielastic scattering can be successfully used for modeling collision cascades in ion-solids collisions. The data obtained clearly indicate that the use of any universal potential is limited to internuclear distances  $R < 7 a_f$  ( $a_f$  is the Firsov length).

## 1. Introduction.

Repulsive interatomic potentials are widely used in plasma physics, astrophysics, surface diagnostics by different types of ion scattering methods, and modeling particle passage through matter. Binary collision approximation and molecular dynamic computer simulations are widely used to describe various types of collision cascades, and the results of such simulations are very sensitive to the choice of the repulsive potential model. This highlights

the importance of being able to determine interatomic potentials accurately either from theory or experiments. Experimental interatomic potential for large interatomic distances were for the first time determined by Amdur and coworkers [1-4, for a review see Ref. 5]. Later important additional contributions were made by Leonas et al. [6], whose measurements provided information on smaller interatomic distances.

The data on the repulsive interaction potentials for close collisions, when the inner shells of colliding atomic particles are involved in the interaction, were obtained in experiments performed by Lane and Everhart [7]. The data processing method proposed by Firsov [8] was for the first time used to obtain the potential values directly from measurements of angular dependence of the scattering cross section.

Later [9] peculiarities in scattering cross-sections were observed, which correlated with inner-shell electron-state vacancy formation in the collisions under study. The model of crossing energy bands was proposed in [10] to explain quantitatively the source of the peculiarities. In Ref. [10] a conclusion concerning the applicability of the model of one-channel or “quasi-elastic” potential for describing scattering of particles with energies of 12–300 keV was also made. The best conformity was obtained with the potential proposed by Csavinszky [11]. Later, systematic measurements of the scattering cross-sections were performed by Loftager and coworkers [12-14]. They also concluded that the measured cross-sections can be fairly well reproduced using the Jensen potential [15] with adjusted parameters, in spite of the fact that inelastic energy losses also occur during the collisions under study.

Many different theoretical methods have been applied to determine potential parameters *ab initio* [14,16-24]. Perhaps the most used potential was the “universal potential” proposed by Ziegler, Biersack and Littmark [17] (hereinafter referred to as the ZBL potential). This potential was obtained by performing an averaging fit to the results of Thomas-Fermi

Preprint of paper published as Nuclear Instruments & Methods B 406 (2017) p. 511-517  
quantum mechanical potential calculations for a large number of systems. The standard deviation of this fit was 18% of the calculated individual potentials [17].

Various theoretical types of potentials were compared in [25] with the set of experimental data on potentials available at that time and obtained mainly for moderate values of collision energy. The authors concluded that the ZBL potential can be applied with relatively high accuracy. Nevertheless, other types of potential (e.g., the Moliere potential [26] and Jensen potential [15]) were used more or less successfully even after publication of paper [25]. Later, more accurate data on the potentials were obtained by the Firsov's method for many ion-atom systems from scattering cross-section measurements [27]. It was shown that the ZBL potential must be improved, and a different functional form was proposed as the best fit of existing experimental data. The results also showed [27] that the range of interatomic distances where any universal potential form can be used is restricted to distances less than  $7 a_f$  (here  $a_f$  is the Firsov's screening length, see below). Later a model of an individual potential was proposed to extend the application area to larger interatomic distances [28]. However, errors in the cases when experimental data are unavailable exceed 15%.

To solve this problem, a set of fully *ab initio* interatomic potential calculations were carried out in Ref. [29], where potentials were calculated using density-functional theory method with Dmol approach for choosing basis wave functions. Although these potentials have been widely used in ion range calculations that were compared to experiments (e.g. Refs. [30-32]), no direct comparison with scattering experiments has been made.

The aim of this paper is to compare the DMol calculations with experimental data and widely used analytical formulae for the repulsive potentials.

## **2. Experimental data on interaction potentials and data processing**

Prior to comparing theoretical calculations and measurements, one should characterize the quality of available experimental data and errors of experiments of different types. First, note

that particles in collisions may be excited and ionized. When particles with kinetic energies of several tens of keV's collide, formation of electron state vacancies in the atom inner shells takes place with additional ionization of the collision partners due to Auger decay of those vacancies. In this case, it is necessary to take into account that scattering is of multichannel character. This is especially important in collisions of light atoms (hydrogen, helium) when ionization or electron capture drastically change the potential curve. Nevertheless, since the inelastic energy losses (including those for ionization) are typically not higher than 6% of the potential at the trajectory turning point, the scattering may be regarded as quasi-elastic, and described via a potential corresponding to the mean inelastic energy loss.

The possibility of using the single-channel potential in describing the scattering process may be checked by comparing data on differential particle scattering cross-sections measured at various initial energies. For convenience, the data on scattering cross-sections at various collision energies are compared in reduced coordinates:  $\rho = \Theta d\sigma/d\Omega \sin\Theta$  and  $\tau = E_{cm} \Theta$ , where  $E_{cm}$  and  $\Theta$  are the collision energy and scattering angle in the center-of-mass system. If the potential is invariant of the particle collision energy, the data in these coordinates may be represented by a common curve independently of the collision energy. Fig. 1 presents data for systems  $Xe^+ - Xe$ ,  $Ar^+ - Ar$  and  $Ne^+ - Ne$  [12-14] in the reduced coordinates. The figure demonstrates that the scattering cross-section – collision energy dependences are not smooth. There are maxima caused by the multi-channel character of the scattering [6]. However, cross-sections at different collision energies differ by no more than 1-3% in the cases under consideration.

To get information on the potential, we use the procedure proposed by Firsov [8]. First the function  $b(\Theta)$  interrelating scattering angle  $\Theta$  and impact parameter  $b$  will be calculated based on the measured cross-sections:

$$b(\Theta) = \{2 \pi \int^{\Theta} d\sigma(\Theta)/d\Omega \sin\Theta d\Theta\}^{1/2}. \quad (1)$$

The inverse function  $\Theta(b)$  can be easily obtained from  $b(\Theta)$ , and then, via the Firsov formula, the potential at the trajectory turning point  $R_o$  reachable at the impact parameter  $b$  will be calculated:

$$U(R_o) = E_{cm} \left( 1 - \exp \left( - b \int_{\Theta}^{\infty} \Theta(b') (b'^2 - b^2)^{-1/2} db' \right) \right), \quad R_o = b \left( 1 - U(R_o)/E_{cm} \right)^{-1/2} \quad (2)$$

An error in absolute cross-section values causes errors in the distance scale calibration for the impact parameter  $b$  and, therefore, for  $R_o$ , of 4%. The errors in relative measurements and angle determination affect the shape of the curve obtained. However, it is worth noting that, due to the integration with respect to  $\Theta$  in calculating  $b(\Theta)$ , the cross-section measurements are being somewhat averaged and, thus, the effect of relative errors decreases to 1-5%.

By using measurements obtained at different energies, it is possible to extend the angular range in the reduced coordinates where the cross-section is known. This will significantly reduce the methodological errors caused by the extrapolation, making them insignificant in a wide range of internuclear distances.

In Amdur method [1-4] the cross-section of particle scattering by the angle lower than the preset one was measured versus the collision energy. The potential shape is postulated: typically, this is a power-law or exponential dependence on the internuclear distance. Potential parameters were obtained by comparison the measurements and simulations using proposed potential form. The errors in the internuclear distance scale calibration were also determined by the accuracy of measuring the gas target density, and were typically about 10%. Methodological errors connected with the assumed shape of the potential curve are difficult to estimate. Nevertheless, these data will be used in comparing with calculations for large  $R$ . A number of experiments at intermediate internuclear distances were carried out by the Leonas [6] group using the Amdur method.

### 3. DMol calculations of interatomic potentials.

In Ref. [29], a methodology was presented where repulsive potentials are calculated using the advanced Hartree-Fock-based and density-functional theory (DFT) methods. DFT method

Preprint of paper published as Nuclear Instruments & Methods B 406 (2017) p. 511-517  
was used to calculate the energy of the electron subsystem of dimer systems at chosen internuclear distances. . The DMol method was chosen since it uses numerically determined basis sets that are not limited to the Gaussian shape. From the comparison of these completely different *ab initio* approaches, it was revealed that using the DMol software with optimization of all orbitals and addition of inner-shell hydrogenic orbitals to the basis sets enables calculating the potentials to better than 1% accuracy above 10 eV, at least for the light and medium-heavy atoms considered [29]. Based on these insights, a script was made that calculated the dimer pair potential for all ion pairs in the atomic number range 1 – 92 with the DMol97 software [33, 34]. Some of the calculations have been checked against the more recent DMol3 version of the software, showing good agreement. For all the atoms, the default orbital basis sets provided with the software were augmented with hydrogenic orbitals. For elements with the atomic number  $Z < 11$  the hydrogenic orbitals were already part of the default DMol97 basis sets, and these were used. For elements with  $10 < Z < 40$ , the hydrogenic orbitals of electron shells 1-4 were added, and also the hydrogenic orbitals of atoms with atomic number  $Z-1$  (following the practice of the default orbitals for  $Z < 11$ ). For elements with  $40 < Z < 55$  hydrogenic orbitals for shells 1-5 were added for  $Z$ , and for shells 1-3 for  $Z-1$ . For elements with  $Z \geq 55$  it was possible to add hydrogenic orbitals only for shells 1-3, since otherwise the maximum number of orbitals allowed by the software was exceeded.

For each atom pair, the dimer energy was calculated for fixed atom coordinates at increasing distance intervals starting from the 0.002 Å interval below 0.1 Å and increasing to an interval of 1.0 Å between 4 and 10 Å. To get the distance at "infinity", also points at the 100 Å and 1000 Å distances were calculated. The dimer energy at 1000 Å separation was used as a subtractive factor to normalize the pair potential to 0 Å at infinity. In total, 74 distance points were used for each dimer pair, which was found to give a smooth description of the pair interaction. The results of our calculations for 19 dimer systems are presented in

Preprint of paper published as Nuclear Instruments & Methods B 406 (2017) p. 511-517  
the table 1. The number of presented distance points is restricted because of limitation of table size.

#### **4. Comparison of DMol calculation with experimental data.**

Fig. 2 shows the comparison for the Ne-Ne system. We have an excellent agreement between theoretical and experimental data [27] for distances less than 1 Å. We have also a good agreement with the Hartung calculations [15]. At  $R < 1$  Å there is a clear disagreement between data from [27] and Leonas's data [6]. We consider the data [6] as much less reliable. At  $R > 1$  Å the data by Leonas [6] and Amdur [2] clearly indicate that calculations by the DMol approach are more accurate than those by Hartung et al [16]. In general, the agreement with experiment is unexpectedly good for the considered case.

Fig 3 shows the data for the Ar-Ar system. As in the case of Ne-Ne, we find an excellent agreement with experimental data [24] and a good agreement with Hartung calculations [14] at  $R < 1$  Å. At  $R > 1$  Å, a reasonable agreement with experimental data by Amdur [1] and Leonas [6] is observed.

Fig 4 illustrates the Kr-Kr case. Here the agreement between the calculations obtained by the DMol method and experimental data is still reasonable. The difference between the calculations and measurements increases with internuclear distance.

Fig 5 presents the data for the Xe-Xe system. The situation is similar to the Kr-Kr case. The difference between the data from [27] and calculations is greater, and the agreement with Leonas's [6] data is worse.

Fig.6 illustrates the comparison of DMol results with experimental data for some asymmetric systems (C-Xe, Ar-Xe and Zn-Xe). The agreement of the results and some trends are the same as for the symmetric systems.

Considering the general trend, we can say that for Ne-Ne and Ar-Ar, the agreement is very good. For heavier elements, the difference between the theory and the experiment increases



Preprint of paper published as Nuclear Instruments & Methods B 406 (2017) p. 511-517 with internuclear distance. This difference could be explained as follows: in the DMol calculations, the total number of orbitals available was limited due to software limitations (see section 3) and, hence, for heavy elements one had to use a smaller number of hydrogenic orbitals. In addition, in case of heavy elements the relativistic effects begin to be important, and DMol only had the lowest-level relativistic correction. In future, calculations with another DFT package that allows using larger numbers of orbitals could be used to improve the theoretical potential calculations.

### 5. Comparison of DMol results with some analytical formulas.

Let us introduce the screening length:

$$a_f = 0.8853 (Z_1^\alpha + Z_2^\alpha)^{-\beta} . \quad (3)$$

Here  $Z_1$  and  $Z_2$  are nuclear charges of colliding particles and atomic units are used. Lindhard et al. [23], Moliere [26] and Jensen [15] used values  $\alpha = 2/3$  and  $\beta = 0.5$ . Firsov [35] suggested that values  $\alpha = 0.5$  and  $\beta = 2/3$  should be better. Ziegler et al. [17] used values  $\alpha = 0.23$  and  $\beta=1$ . Here we will use the values offered by Firsov. Let us rewrite the potential in the following form:

$$U(R) = Z_1 Z_2 / (x a_f) \exp\{-B(x) x\}, \quad x = R / a_f. \quad (4)$$

Fig. 6 shows the results of comparing the calculations obtained using the DMol approach with data obtained with the Moliere, Jensen and ZBL potentials. In Ref. [27] a different functional form of  $B(x)$  was proposed:

$$B(x) = c_1 / (1 + c_2 x^{1/2} + c_3 x), \quad (5)$$

Parameters  $c_1 = 1.575$ ,  $c_2 = 0.719$ ,  $c_3 = -0.010$  were selected as the best "universal" fit of experimental data [28]. In [28], parameters  $c_1$ ,  $c_2$ ,  $c_3$  are also given for each of the studied systems. The results of this fit are also shown in Fig. 7 as the Zinoviev potential. One can see that the Moliere potential data are generally higher than the DMol calculations, while the

Jensen and ZBL potentials are lower. The Zinoviev fit is the middle of the DMol calculations.

Fig.7 shows that the data spread at  $x > 7$  is sufficiently high.

The potential data for different systems vary by many orders of magnitude. The screening parameter  $B(x) = -\ln \{U(x) \times a_f / (Z_1 Z_2)\} / x$  changes slowly. In the case of the Bohr potential,  $B(x)$  is constant. It is more convenient to use this function for the analysis, because the Coulomb term and exponential dependence on  $x$  are eliminated in this case. Therefore, it allows clearly demonstrating any deviations from the screened Coulomb potential. The function  $B(x)$  values obtained by the DMol calculations are shown in Fig. 8. On average, the agreement with the proposed fit [28] is satisfactory, keeping in mind that this fit represents an average of the experimental data. There is some difference at small  $x$ , which implies that the set of united atom orbitals used in the DMol approach is probably not sufficiently large. These deflections do not influence strongly on the potential value because of the dominant contribution of the nuclear interaction term at these distances.

Table 2 shows the mean standard deviations of potentials  $\delta U$  calculated by the DMol method and corresponding screening functions  $\delta B$  relative to the universal values given by potential [28] as a function of internuclear distance  $x$ . At  $x > 7$ , the error in the potential estimation performed by using the universal potential exceeds 50%. Therefore, the region of application of the universal potential is limited to  $x < 7$ .

## 7. Conclusions.

In this paper, we compared interatomic potentials calculated with the DFT DMol approach with experiments and theory. The results showed that the DMol approach allows obtaining quite reasonable data for modeling different collisions. The agreement with the experiment is excellent for light collision partners and quite satisfactory for heavier atoms. The quality of calculations can be improved by extending the basis set. The experimental data proves that the approach of quasielastic scattering can be successfully used in modeling collision cascades in

Preprint of paper published as Nuclear Instruments & Methods B 406 (2017) p. 511-517  
ion-solids collisions. Moreover, analysis of the obtained data shows that the application region  
of any universal repulsive potential is restricted to  $R < 7 a_f$ . The fit proposed in [28] can be  
recommended for potential estimations.

**References.**

1. I. Amdur, E.A. Mason, *J.Chem.Phys.* 22 (1954) 670.
2. I. Amdur, E.A. Mason, *J.Chem.Phys.* 23 (1955) 415;
3. I. Amdur, E.A. Mason, *J.Chem.Phys.* 23 (1955), 2268;
4. I. Amdur, E.A. Mason, *J.Chem.Phys.* 25 (1956) 624.
5. E.A. Mason, J.T. Vanderslice, in *Atomic and Molecular Processes*, ed. D.R. Bates, (Academic press, N.Y. 1962), p.663-692.
6. V. Leonas, *Uspekhi Fiz.Nauk*, 107 (1972) 29.
7. G.H. Lane, E. Everhart, *Phys. Rev.* 120 (1960) 2064.
8. O.B. Firsov, *JETP* 33 (1957) 696.
9. V.V. Afrosimov, Yu.S. Gordeev, V.K. Nikulin, A.M. Polanskii, A.P. Shergin *JETP*, 35 (1972) 449.
10. V.V. Afrosimov, Yu.S. Gordeev, A.N. Zinov'ev, *JETP* 66 (1974) 1933.
11. P. Csavinszky, *Phys. Rev.* 166 (1968) 53.
12. P. Loftager, F. Besebbacher, O.S. Jensen, V.S. Sorensen, *Phys. Rev. A*20 (1979) 1443.
13. P. Loftager. G. Claussen, *Abstr. YI ICPEAC*, Cambridge, 1969, p. 518.
14. H. Hartung, B. Fricke, W.-D.Sepp. et al. *Phys. Lett.* 119 (1987) 457.
15. H.Z. Jensen, *Phys. B* 18 (1932) 722
16. H. Hartung, B. Fricke, W.-D.Sepp., W.Sengler, D.Kolb, *J. Phys. B.* 1985. Vol. 18. L433.
17. J.F. Ziegler, J.P. Biersack, U. Littmark, *The Stopping and Range of Ions in Solids.* v1, Pergamon Press, N.Y. (1983).
18. W. Eckstein, S.Yaskel, D.Heinemann, B. Fricke, *Z.Phys.D* 24 (1992) 171
19. V.I. Gaydaenko, V.K. Nikulin, *Chem. Phys. Lett.* 7 (1970) 360.
20. Y.S. Kim, R.G. Gordon, *J.Chem.Phys.* 60 (1974) 4323
21. E.J.J. Kirchner, E.A. Baerends, U.van Slooten, A.W.Klein, *J.Chem.Phys.* 97 (1992) 3821
22. D.E. Harrison Jr., P. Avouris, R. Walkrup, *Nucl. Instr. Meth. Phys. Res.* B18 (1987) 349

Preprint of paper published as Nuclear Instruments & Methods B 406 (2017) p. 511-517

23. J. Linchard, V. Nielsen, M. Scharff, K. Danske Vidensk. Selsk. Mat. Fys. Medd. 36 (1986) N 10.
24. A. Dygo, A. Tuross, Nucl.Instr.Meth. Phys. Res. B18 (1987) 349
25. D. J. O'Connor, J.E. Biersack Nucl. Instr. Meth. Phys. Res. B15 (1986) 14.
26. G. Moliere, Zs. Naturforsch. 1949. Bd 2a (1949) 133.
27. A.N. Zinoviev, Tech.Phys. 53 (2008) 13.
28. A.N. Zinoviev, Nucl. Instr. Meth. Phys. Res. B 269 (2011) 829.
29. K. Norlund, N. Runeberg, D. Sundholm, Nucl. Instr. Meth. Phys. Res. 132 (1997) 45.
30. P. Oldiges, H. Zhu, and K. Nordlund, Proceedings of the 1997 International Conference on Simulation of Semiconductor Processes and Devices (SISPAD) (IEEE, USA, 1997), p. 245-247.
31. J. Sillanpää, K. Nordlund, and J. Keinonen, Phys. Rev. B 62 (2000) 3109.
32. J. Peltola, K. Nordlund, and J. Keinonen, Nucl. Instr. Meth. Phys. Res. B 212 (2003) 118.
33. J. Delley, J. Chem. Phys., 92: (1990) 508.
34. DMol software, 1997 version. DMol is a trademark of AccelRys. Inc.
35. O.B. Firsov, JETP, 34 (1958) 447.

R	Ar-Al	Ar-Ag	Ar-Ar	Ar-Xe	C-Xe	Kr-Al	Kr-Ar	Kr-C	Kr-Ge	Kr-Kr
0,002	1,65E+06	5,95E+06	2,30E+06	6,82E+06	2,28E+06	3,30E+06	4,56E+06	1,52E+06	8,12E+06	9,13E+06
0,004	8,12E+05	2,91E+06	1,13E+06	3,33E+06	1,11E+06	1,61E+06	2,23E+06	7,46E+05	3,97E+06	4,47E+06
0,01	3,08E+05	1,09E+06	4,30E+05	1,25E+06	4,19E+05	6,08E+05	8,41E+05	2,82E+05	1,49E+06	1,68E+06
0,014	2,13E+05	7,50E+05	2,98E+05	8,56E+05	2,88E+05	4,18E+05	5,79E+05	1,94E+05	1,02E+06	1,15E+06
0,02	1,42E+05	4,96E+05	1,99E+05	5,65E+05	1,91E+05	2,78E+05	3,84E+05	1,29E+05	6,76E+05	7,60E+05
0,04	6,14E+04	2,08E+05	8,56E+04	2,36E+05	8,09E+04	1,18E+05	1,62E+05	5,53E+04	2,82E+05	3,16E+05
0,08	2,37E+04	7,72E+04	3,24E+04	8,69E+04	3,05E+04	4,43E+04	6,05E+04	2,11E+04	1,03E+05	1,15E+05
0,1	1,69E+04	5,38E+04	2,29E+04	6,06E+04	2,14E+04	3,11E+04	4,24E+04	1,49E+04	7,16E+04	7,98E+04
0,14	9,72E+03	3,00E+04	1,30E+04	3,35E+04	1,21E+04	1,74E+04	2,37E+04	8,45E+03	3,94E+04	4,37E+04
0,16	7,65E+03	2,33E+04	1,01E+04	2,59E+04	9,57E+03	1,37E+04	1,86E+04	6,60E+03	3,04E+04	3,37E+04
0,2	4,98E+03	1,47E+04	6,57E+03	1,64E+04	6,27E+03	8,99E+03	1,20E+04	4,30E+03	1,91E+04	2,14E+04
0,24	3,41E+03	9,93E+03	4,55E+03	1,12E+04	4,30E+03	6,16E+03	8,04E+03	3,00E+03	1,30E+04	1,47E+04
0,32	1,84E+03	5,22E+03	2,48E+03	5,80E+03	2,30E+03	3,13E+03	4,10E+03	1,64E+03	6,55E+03	7,48E+03
0,4	1,13E+03	2,92E+03	1,42E+03	3,29E+03	1,39E+03	1,77E+03	2,39E+03	9,27E+02	3,64E+03	4,09E+03
0,5	6,11E+02	1,57E+03	7,88E+02	1,87E+03	7,74E+02	9,89E+02	1,26E+03	4,93E+02	1,89E+03	2,19E+03
0,6	3,55E+02	9,34E+02	4,87E+02	1,10E+03	4,47E+02	5,68E+02	7,20E+02	2,89E+02	1,08E+03	1,19E+03
0,7	2,23E+02	5,63E+02	3,25E+02	6,69E+02	2,71E+02	3,36E+02	4,51E+02	1,81E+02	5,99E+02	6,80E+02
0,8	1,50E+02	3,38E+02	2,18E+02	4,33E+02	1,74E+02	2,12E+02	2,99E+02	1,14E+02	3,53E+02	4,25E+02
0,9	1,05E+02	2,10E+02	1,44E+02	2,92E+02	1,15E+02	1,42E+02	2,03E+02	7,09E+01	2,22E+02	2,83E+02
1	7,40E+01	1,35E+02	9,64E+01	2,03E+02	7,54E+01	9,83E+01	1,39E+02	4,37E+01	1,46E+02	1,94E+02
1,2	3,45E+01	5,84E+01	4,85E+01	1,02E+02	3,09E+01	4,84E+01	6,92E+01	1,62E+01	6,58E+01	9,76E+01
1,4	1,54E+01	2,58E+01	2,77E+01	5,32E+01	1,18E+01	2,32E+01	3,81E+01	5,82E+00	3,00E+01	5,34E+01
1,6	7,02E+00	1,13E+01	1,47E+01	2,90E+01	4,02E+00	1,10E+01	2,04E+01	1,86E+00	1,36E+01	2,87E+01
2	1,56E+00	2,08E+00	3,92E+00	8,76E+00	-2,87E-01	2,55E+00	5,75E+00	-2,58E-01	2,56E+00	8,32E+00
2,2	7,19E-01	8,45E-01	1,88E+00	4,71E+00	-6,50E-01	1,19E+00	2,90E+00	-2,62E-01	9,43E-01	4,35E+00
2,4	2,88E-01	3,04E-01	8,48E-01	2,45E+00	-4,97E-01	5,06E-01	1,39E+00	-1,92E-01	2,78E-01	2,19E+00
2,6	7,01E-02	6,98E-02	3,45E-01	1,21E+00	-3,76E-01	1,55E-01	6,24E-01	-1,67E-01	1,29E-01	1,05E+00
3	-1,60E-02	-6,00E-02	1,50E-02	2,26E-01	-2,31E-01	-3,21E-02	7,27E-02	-1,23E-01	-3,40E-02	1,75E-01

Table 1. Potential values calculated using Dmol approach (R in Angstrom, U in eV)

R	Kr-N	Kr-Ne	Kr-Si	Kr-Xe	N-Xe	Ne-Ne	Ne-Xe	Xe-Xe	Zn-Xe
0,002	1,78E+06	2,54E+06	3,55E+06	1,36E+07	2,66E+06	7,09E+05	3,79E+06	2,04E+07	1,14E+07
0,004	8,70E+05	1,24E+06	1,74E+06	6,65E+06	1,30E+06	3,49E+05	1,85E+06	9,96E+06	5,54E+06
0,01	3,28E+05	4,68E+05	6,54E+05	2,48E+06	4,88E+05	1,33E+05	6,95E+05	3,70E+06	2,07E+06
0,014	2,26E+05	3,22E+05	4,50E+05	1,69E+06	3,35E+05	9,24E+04	4,77E+05	2,53E+06	1,41E+06
0,02	1,51E+05	2,14E+05	2,99E+05	1,11E+06	2,22E+05	6,19E+04	3,15E+05	1,65E+06	9,30E+05
0,04	6,43E+04	9,10E+04	1,26E+05	4,59E+05	9,41E+04	2,70E+04	1,33E+05	6,75E+05	3,86E+05
0,08	2,45E+04	3,44E+04	4,75E+04	1,65E+05	3,54E+04	1,05E+04	4,98E+04	2,40E+05	1,40E+05
0,1	1,74E+04	2,43E+04	3,33E+04	1,14E+05	2,48E+04	7,45E+03	3,49E+04	1,65E+05	9,67E+04
0,14	9,78E+03	1,36E+04	1,87E+04	6,16E+04	1,40E+04	4,27E+03	1,96E+04	8,90E+04	5,24E+04
0,16	7,65E+03	1,07E+04	1,47E+04	4,78E+04	1,10E+04	3,43E+03	1,54E+04	6,84E+04	4,05E+04
0,2	4,99E+03	7,03E+03	9,60E+03	3,03E+04	7,18E+03	2,38E+03	9,86E+03	4,29E+04	2,59E+04
0,24	3,50E+03	4,87E+03	6,54E+03	2,02E+04	4,91E+03	1,71E+03	6,71E+03	2,91E+04	1,74E+04
0,32	1,86E+03	2,50E+03	3,31E+03	1,02E+04	2,64E+03	9,15E+02	3,61E+03	1,49E+04	8,70E+03
0,4	1,04E+03	1,41E+03	1,89E+03	5,71E+03	1,59E+03	5,15E+02	2,14E+03	8,66E+03	4,98E+03
0,5	5,53E+02	7,69E+02	1,05E+03	3,05E+03	8,73E+02	2,71E+02	1,18E+03	4,90E+03	2,63E+03
0,6	3,23E+02	4,55E+02	5,97E+02	1,79E+03	4,99E+02	1,59E+02	6,89E+02	2,88E+03	1,49E+03
0,7	1,98E+02	2,71E+02	3,56E+02	1,07E+03	3,01E+02	1,06E+02	4,27E+02	1,75E+03	9,03E+02
0,8	1,20E+02	1,63E+02	2,28E+02	6,57E+02	1,91E+02	7,78E+01	2,67E+02	1,07E+03	5,46E+02
0,9	7,17E+01	1,02E+02	1,54E+02	4,23E+02	1,23E+02	5,68E+01	1,65E+02	6,64E+02	3,29E+02
1	4,20E+01	6,72E+01	1,06E+02	2,85E+02	7,70E+01	3,69E+01	1,04E+02	4,31E+02	2,06E+02
1,2	1,37E+01	3,29E+01	4,99E+01	1,41E+02	2,82E+01	1,45E+01	4,52E+01	2,03E+02	8,89E+01
1,4	3,79E+00	1,72E+01	2,26E+01	7,45E+01	8,96E+00	5,53E+00	2,26E+01	1,06E+02	4,16E+01
1,6	3,64E-01	8,68E+00	1,00E+01	4,14E+01	1,74E+00	2,04E+00	1,19E+01	5,98E+01	2,02E+01
2	-4,90E-01	1,88E+00	1,73E+00	1,25E+01	-1,19E+00	2,10E-01	3,11E+00	1,89E+01	5,00E+00
2,2	-3,59E-01	7,99E-01	5,47E-01	6,87E+00	-9,20E-01	3,68E-02	1,48E+00	1,07E+01	2,62E+00
2,4	-3,03E-01	3,04E-01	1,10E-01	3,68E+00	-7,01E-01	-1,48E-02	6,55E-01	5,96E+00	1,39E+00
2,6	-2,55E-01	9,04E-02	4,50E-02	1,91E+00	-5,46E-01	-2,41E-02	2,58E-01	3,25E+00	7,15E-01
3	-1,55E-01	-2,13E-02	-5,44E-02	4,23E-01	-3,25E-01	-1,48E-02	3,91E-03	8,61E-01	1,39E-01

Table 1. (Continuation)

Table 2. The standard deviations of individual potentials  $\delta U$  calculated by the DMol approach and corresponding screening functions  $\delta B$  relative to universal values given by potential [28] as a function of internuclear distance  $x$ .

X	0.1	0.2	0.5	1	2	3	5	7	10
$\delta B$	0.074	0.049	0.033	0.033	0.034	0.045	0.055	0.063	0.11
$\delta U$	0.007	0.010	0.016	0.034	0.070	0.15	0.32	0.55	0.80



## Captions

Fig. 1. Scattering cross sections in reduced units (see the text).

Fig. 2. Interaction potential for  $\text{Ne}^+\text{-Ne}$ . The Amdur's data [2] were obtained for the Ne-Ne (atom-atom) system.

Fig. 3. Interaction potential for  $\text{Ar}^+\text{-Ar}$ . The Amdur's data [1] are presented for the Ar-Ar system.

Fig. 4. Interaction potential for  $\text{Kr}^+\text{-Kr}$ . The Amdur's data [3,] were obtained for the Kr-Kr system.

Fig. 5. Interaction potential for  $\text{Xe}^+\text{-Xe}$ . The Amdur's data [4] are presented for the Xe-Xe system.

Fig. 6. Interaction potential for asymmetric systems (C-Xe, Ar-Xe, Zn-Xe). Data for Ar-Xe were multiplied by a factor of 3 to make the picture clearer.

Fig. 7. Interaction potentials calculated using the DMol approach as compared with the potentials proposed by Moliere [26], ZBL [17], Jensen [15] and Zinoviev [28]. The Ne-Kr data coincides almost exactly with the ZBL data for the same system and hence is not visible in the figure.

Fig. 8. Screening function  $B(x)$  versus scaled internuclear distance  $x$ . Points are the DMol calculations for different systems. The solid line is function  $B(x)$  proposed in [28].

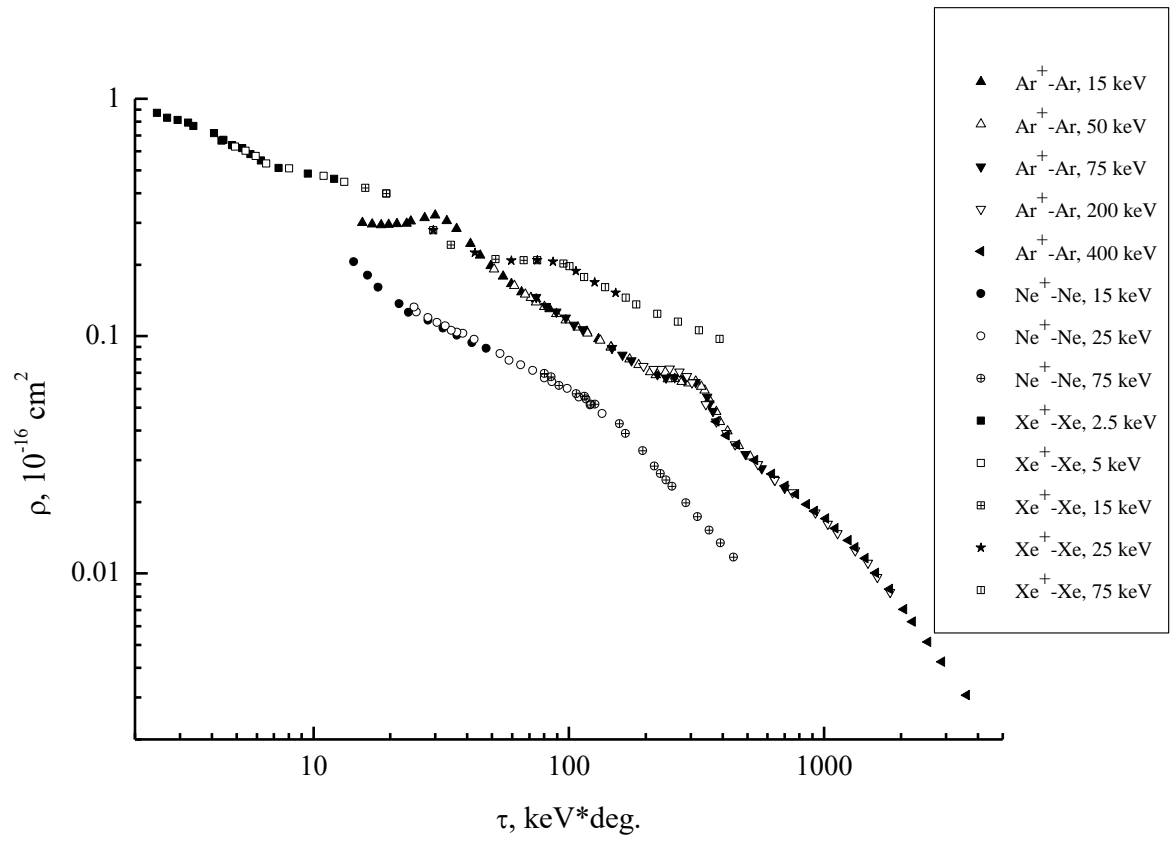


Fig.1

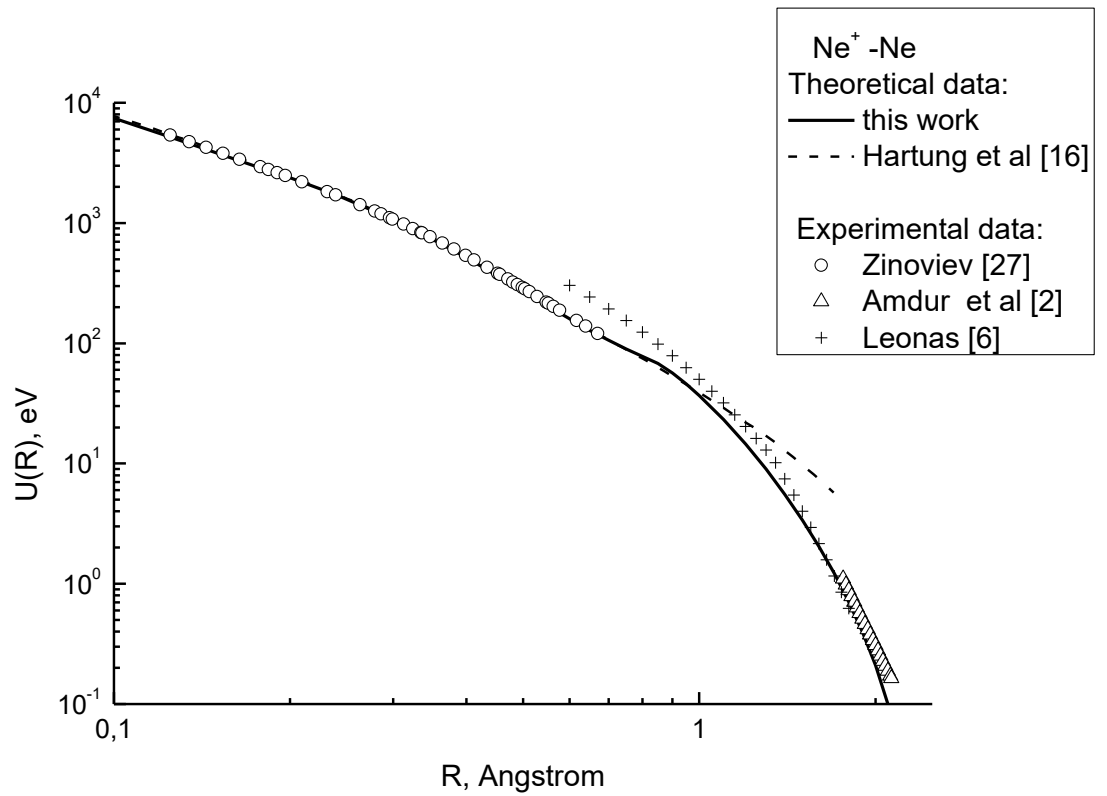


Fig.2

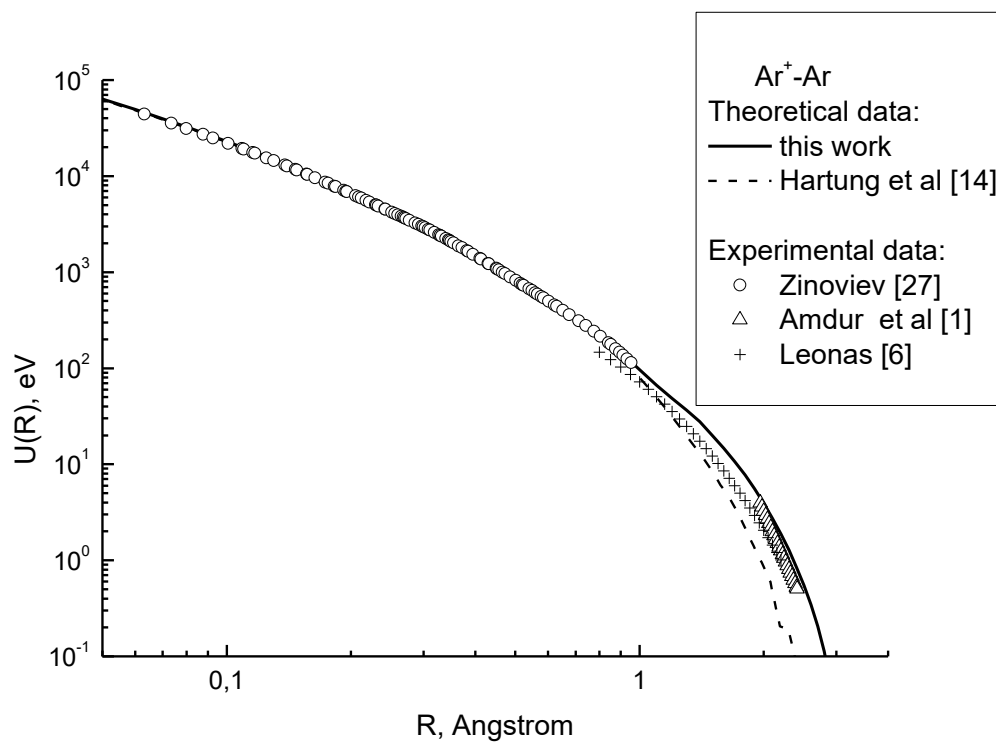


Fig.3

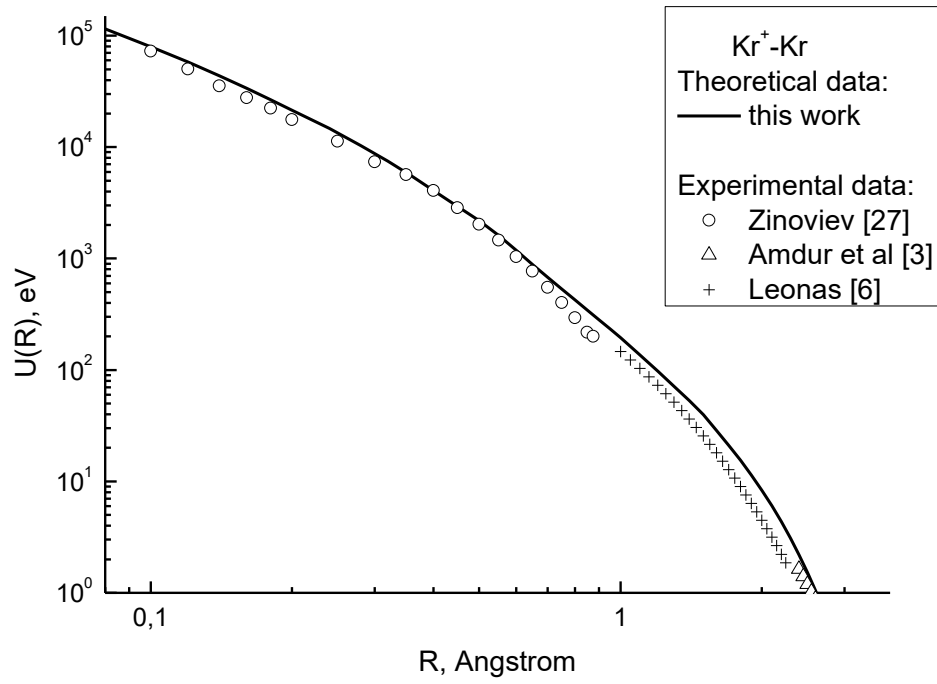


Fig.4

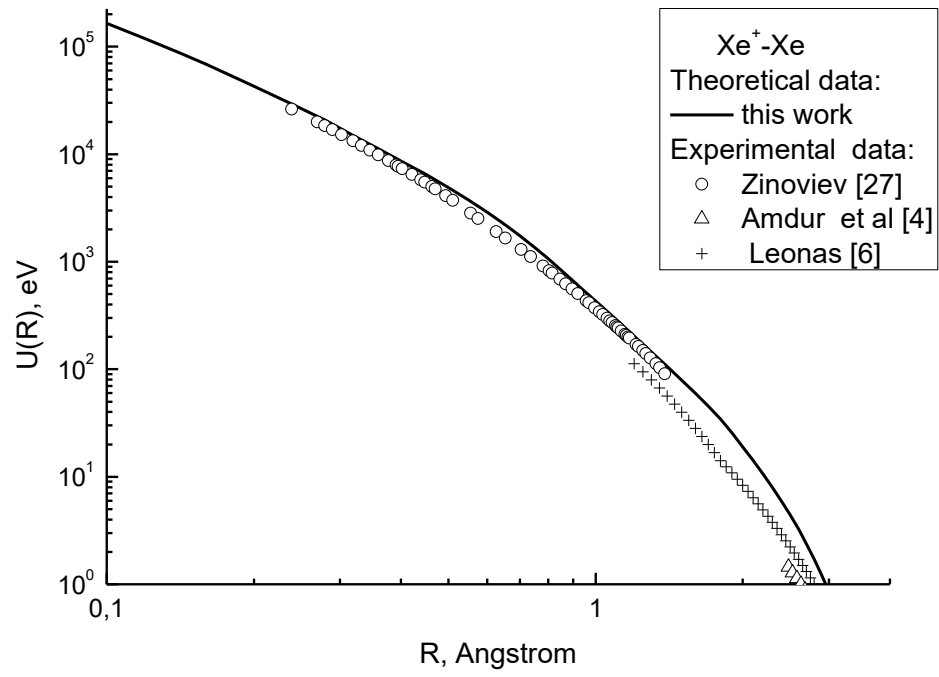


Fig.5

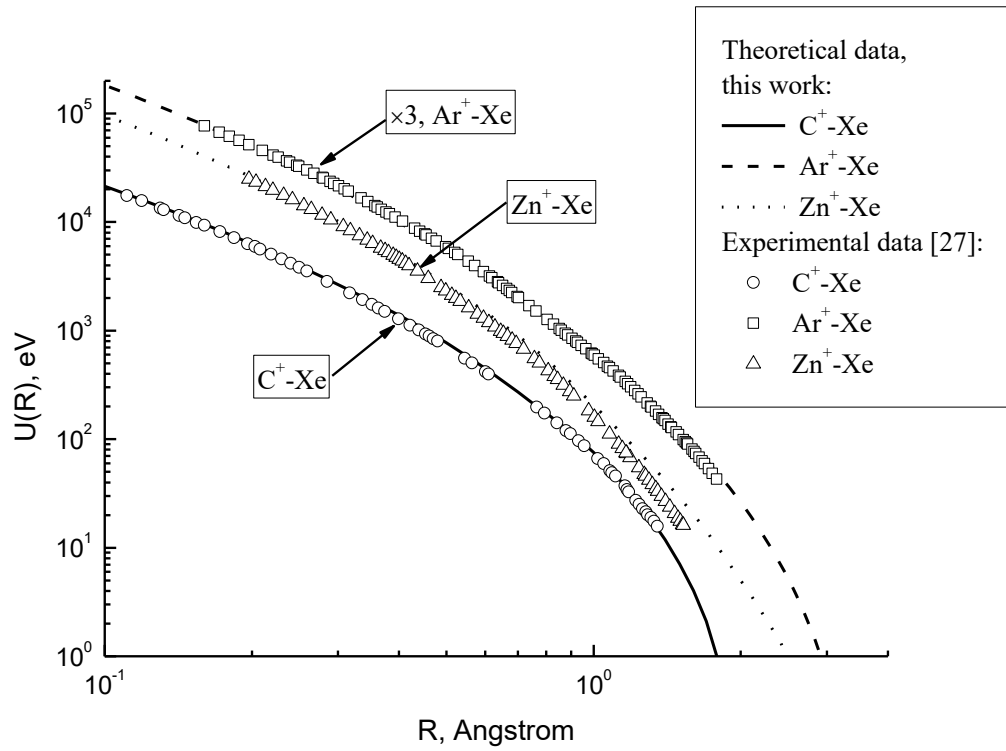


Fig. 6.

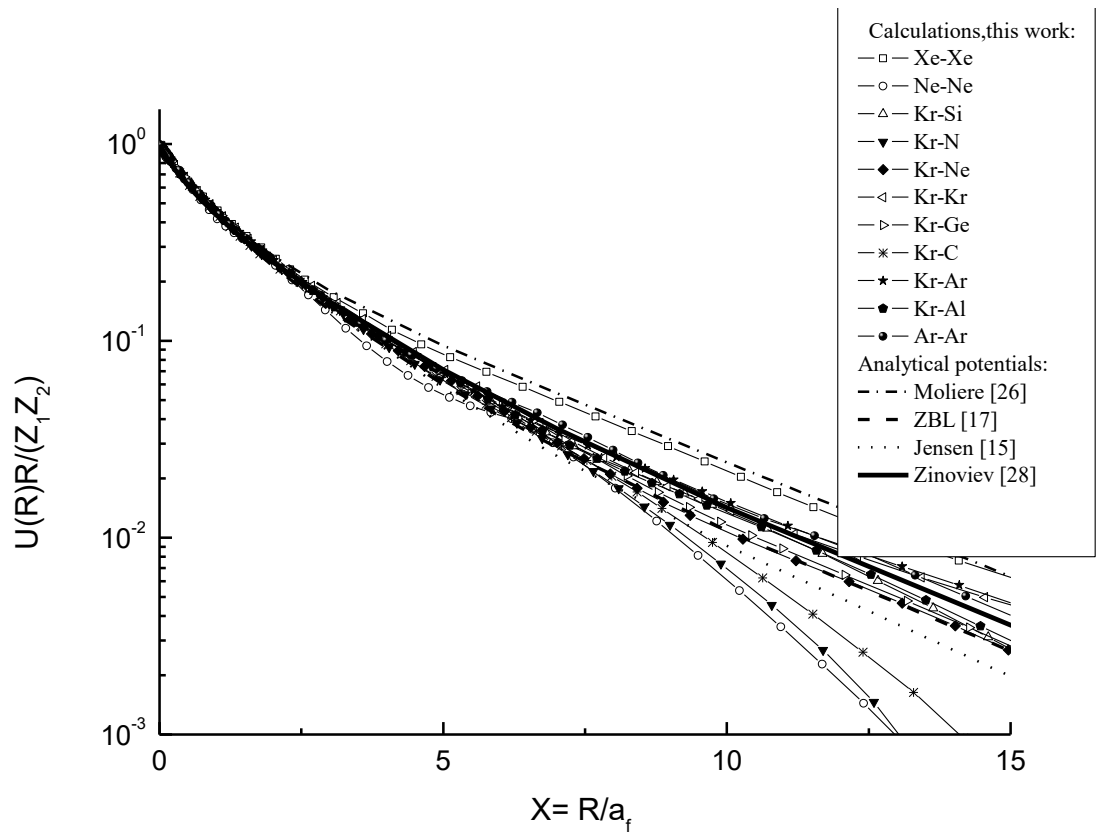


Fig.7



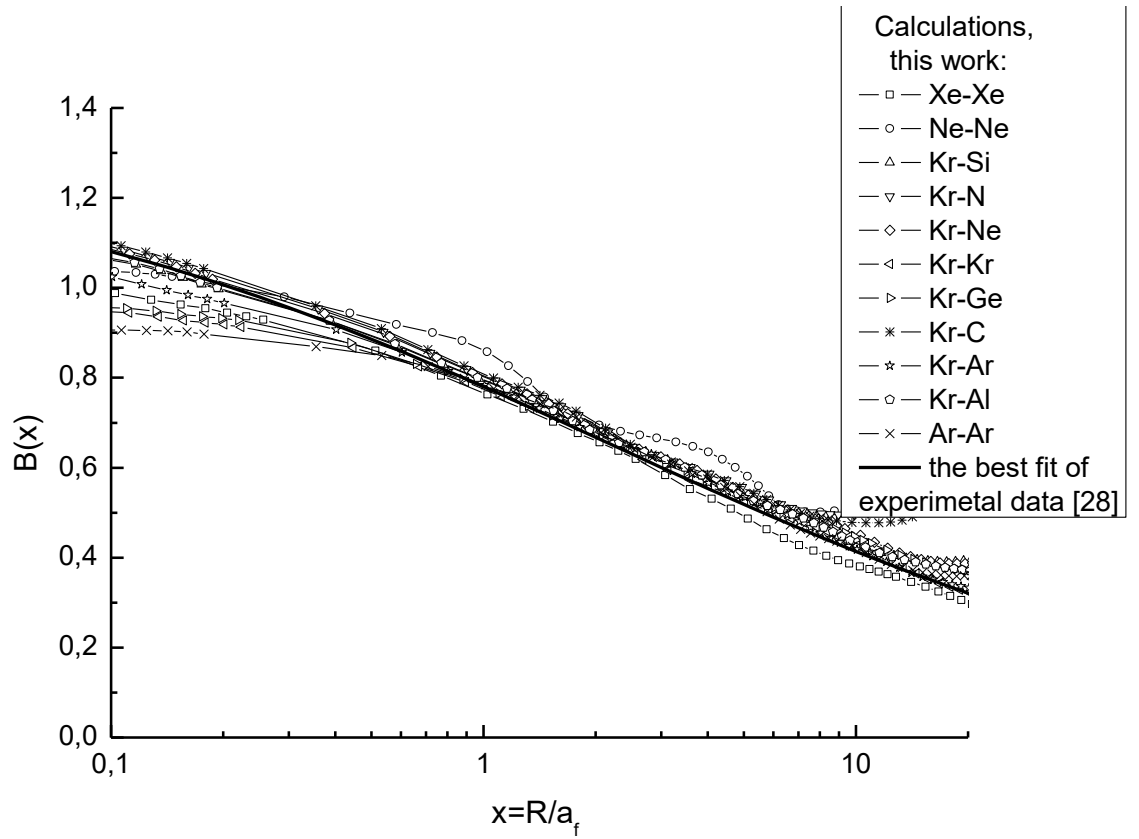


Fig. 8.

